



HAL
open science

Potash fertilizer promotes incipient salinization in groundwater irrigated semi-arid agriculture

Sriramulu Buvaneshwari, Jean Riotte, Muddu Sekhar, Amit Kumar Sharma, Rachel Helliwell, M. Kumar, J. Braun, Laurent Ruiz

► **To cite this version:**

Sriramulu Buvaneshwari, Jean Riotte, Muddu Sekhar, Amit Kumar Sharma, Rachel Helliwell, et al.. Potash fertilizer promotes incipient salinization in groundwater irrigated semi-arid agriculture. *Scientific Reports*, 2020, 10 (1), <10.1038/s41598-020-60365-z>. <hal-03190864>

HAL Id: hal-03190864

<https://hal.inrae.fr/hal-03190864v1>

Submitted on 7 Apr 2021

HAL is a multi-disciplinary open access archive for the deposit and dissemination of scientific research documents, whether they are published or not. The documents may come from teaching and research institutions in France or abroad, or from public or private research centers.

L'archive ouverte pluridisciplinaire **HAL**, est destinée au dépôt et à la diffusion de documents scientifiques de niveau recherche, publiés ou non, émanant des établissements d'enseignement et de recherche français ou étrangers, des laboratoires publics ou privés.



Distributed under a Creative Commons CC BY-ND 4.0 - Attribution - No Derivative Works - International License

OPEN

Potash fertilizer promotes incipient salinization in groundwater irrigated semi-arid agriculture

Sriramulu Buvaneshwari^{1,2,6,7*}, Jean Riotte^{2,3}, Muddu Sekhar^{1,2}, Amit Kumar Sharma^{2,5}, Rachel Helliwell⁶, M. S. Mohan Kumar^{1,2}, J. J. Braun³ & Laurent Ruiz^{2,3,4}

Incipient groundwater salinization has been identified in many arid and semi-arid regions where groundwater is increasingly used for irrigation, but the dominant processes at stake in such context are yet uncertain. Groundwater solutes originates from various sources such as atmospheric inputs, rock dissolution and fertilizer residues, and their concentration is controlled by hydrological processes, in particular evapotranspiration. Here, we propose a deconvolution method to identify the sources and processes governing the groundwater Chloride concentration in agricultural catchments, using the relative variations of Sodium and Chloride and using a neighbouring pristine catchment as a reference for the release rate of Na by weathering. We applied the deconvolution method to the case of the Kabini Critical Zone Observatory, South India, where groundwater was sampled in 188 farm tubewells in the semi-arid catchment of Berambadi and in 5 piezometers in the pristine catchment of Mule Hole. In Berambadi, groundwater composition displayed a large spatial variability with Cl contents spanning 3 orders of magnitude. The results showed that the concentration factor due to evapotranspiration was on average about 3 times more than in the natural system, with higher values in the valley bottoms with deep Vertisols. Linked with this process, large concentration of Chloride originating from rain was found only in these areas. At the catchment scale, about 60 percent of the Chloride found in groundwater originates from fertilizer inputs. These results show that Potassium fertilization as KCl is an important source of groundwater salinization in semi-arid context, and stress that identifying dominant drivers is crucial for designing efficient mitigation policies.

Groundwater salinization is a growing global concern¹. The general processes leading to salinization are well understood since a long time² with causes being either natural, anthropogenic or a mix of the two³. Indeed, most of the literature has been focused on areas prone to widespread salinization, such as coastal areas prone to seawater intrusion⁴⁻⁶, groundwater irrigation from aquifers bearing evaporites⁷, command areas of dams where waterlogging restrict salt leaching⁸ or arid areas where historical accumulation of salts in the deep vadose zone due to evapotranspiration can be leached when natural vegetation is replaced by agriculture⁹. However, even in the absence of such adverse conditions, risks of groundwater recharge salinization have been identified in many arid and semi-arid regions where groundwater is increasingly used for irrigation¹⁰⁻¹³. As in these situations the attention is directed towards water resource depletion issues, this incipient salinization has been scantily studied¹⁴. As of now, the extent of the problem and its spatial variability is hardly documented and designing sustainable management practice to mitigate it is challenging because the relative contributions of the potential processes at stake are difficult to assess.

Salts in the soil naturally originate from precipitation and mineral dissolution. Their concentrations are primarily linked to the ratio between evapotranspiration (ET) and precipitation (P), explaining why high salt concentrations in soils are mainly found in arid and semi-arid regions⁹. Chlorine is one of the most abundant elements in rain water, but is rarely present in primary minerals, except from evaporites. This feature, combined with its conservative behaviour, makes it a useful tracer of water balance, and it has been widely used to estimate groundwater recharge with Chloride Mass Balance (CMB) method¹⁵⁻²¹. Like Chlorine, Sodium is abundant in

¹Indian Institute of Science, Bangalore, India. ²Indo-French Cell for Water Sciences, Indian Institute of Science, Bangalore, India. ³IRD, CNRS, UPS, UMR GET, Toulouse, France. ⁴INRAE, AGROCAMPUS OUEST, UMR SAS, Rennes, France. ⁵Univ Rennes, CNRS, UMR LETG, Rennes, France. ⁶James Hutton Institute, Aberdeen, United Kingdom. ⁷Present address: ICWaR, Indian Institute of Science, Bangalore, India. *email: buvaneshwaris@iisc.ac.in

rain water, but it is also released by Na-plagioclase weathering^{22,23}. The Na/Cl ratio is therefore widely used to characterize water types, with surface waters being close to marine ratio (0.86) while water having much higher ratios indicate long residence time in weathering material^{7,24–26}.

In agrosystems, salts are also often added by fertilizers. In many agrosystems Cl is widely applied as potash, i.e. in the form of KCl²⁷. Amongst the mineral fertilizers, KCl has the highest impact on soil salinity because K is efficiently taken up and exported by plants as a macronutrient while Cl, which is a micro-nutrient²⁸ remains in soil pore water and concentrates through evapotranspiration. Chloride toxicity is commonly observed in arid and semiarid regions where improper irrigation practices²⁹ and high evaporation rates can lead salt accumulation in soils³⁰. To the contrary, Na is rarely present in chemical fertilizers since nitrogen fertilization with NaNO₃ was abandoned in the early twentieth century³¹. Therefore, in intensive agrosystems, fertilizer addition might affect the interpretation of Na/Cl ratios and the estimation of recharge with CMB.

Agriculture is also impacting the salt concentration in soil, by modifying evapotranspiration (ET) rates. Rainfed agriculture, with long periods of bare soils, has usually a lower ET than natural vegetation, leading to diluted soil water concentrations⁹. To the contrary, irrigation increases ET by allowing longer crop cycles and denser canopies, leading to increased salt concentration in soil pore water. In the case of GW irrigation, recycling of salts is likely to worsen this problem^{32–34}.

In India, increasing groundwater irrigated area has allowed to sustain the growth of agricultural production since 40 years and to meet the need of a growing population^{11,35}. In the Deccan plateau in South India, the development of submersible pump technology allowed millions of small farmers, typically holding about 1 ha of land, to access irrigation through tubewells in a region previously dominated by rainfed agriculture³⁶. The resulting high diversity of cropping systems and irrigation techniques is likely to induce a large variability in groundwater recharge composition. For instance, the variability of groundwater contamination by nitrates was revealed at the scale of a small agricultural watershed from high density tubewell monitoring and attributed to the heterogeneity of aquifer properties and farming practices³⁷. In the same site³⁸, showed that incipient groundwater salinization was already significantly affecting crop yields, but the processes driving the spatial variations of salinization in groundwater have still to be documented.

Existing approaches to identify hydro chemical processes in groundwater are poorly adapted to such a context, characterized by high small-scale spatial heterogeneity. Geochemical analysis³⁹ (e.g. piper diagram or multivariate analysis) are well suited for large aquifers, where large scale spatial heterogeneity in geological substrate or land use create strongly differentiated geochemical signatures in groundwater. Similarly, geochemical tracers, like isotopes, are widely used^{40,41}. Although being more quantitative, they also need a strong spatial signal (e.g. altitudinal gradient in the case of water isotopes). Using mechanistic modelling would be suitable, and a wide range of models exist⁴² but it would require gathering large datasets to parametrize such heterogeneous systems. Deconvolution methods are classically used to identify the origin of solutes in rivers^{25,43–47} and Na/Cl ratio is commonly used to assess the respective contributions of atmospheric vs geogenic sources of solutes and estimate silicate weathering and particularly Na-plagioclase weathering⁴⁸. However, the contribution of fertilizer inputs is usually neglected in such studies.

As the consequence, identifying and quantifying the sources and processes driving salinization in groundwater irrigated agrosystems remains a challenge. In this paper, we propose to combine data from an agricultural catchment (Berambadi) and a neighbouring pristine forested catchment (Mule Hole), both belonging to the Kabini Critical Zone Observatory in South India⁴⁹ to (i) explore the spatial variability of groundwater chemical composition based on high density tubewell sampling and (ii) quantify the concentration factor (CF) due to Evapotranspiration (ET) and estimate the relative contribution of rainfall vs fertilizer addition to Cl total input in agrosystems.

Rationale of the Deconvolution Method

In agrosystems, solutes originate from atmospheric inputs, mineral weathering and fertilizer residues, and their concentration in groundwater increase with the effect of evapotranspiration. In our method, we propose to deconvolute groundwater Chloride concentrations using Na as a reference to assess the contribution of fertilizers to incipient salinization in agricultural catchments.

In a natural system, the only source of Cl is rain^{47,50,51} and therefore we can write:

$$[\text{Cl}]_{\text{G}} = [\text{Cl}]_{\text{G(R)}} \quad (1)$$

where $[\text{Cl}]_{\text{G}}$ = Chloride concentration in groundwater (μmolL^{-1}), $[\text{Cl}]_{\text{G(R)}}$ = concentration in groundwater of Chloride originating from rain input (μmolL^{-1}).

As Cl is conservative in the system and plant uptake is negligible, the ratio between the Cl concentration in groundwater and in the rain can be used to estimate the concentration factor due to ET⁵² (CF, dimensionless). For a given tubewell, we can write:

$$\text{CF} = \frac{[\text{Cl}]_{\text{G}}}{[\text{Cl}]_{\text{R}}} \quad (2)$$

where $[\text{Cl}]_{\text{R}}$ = Chloride concentration in rain (μmolL^{-1})

For Na, as it is added both by the rain and by mineral weathering, we can write

$$[\text{Na}]_{\text{G}} = [\text{Na}]_{\text{G(R)}} + [\text{Na}]_{\text{G(w)}} \quad (3)$$

where $[\text{Na}]_G$ = Sodium concentration in groundwater (μmolL^{-1}), $[\text{Na}]_{G(R)}$ = Concentration in groundwater of Sodium originating from rain input (μmolL^{-1}), $[\text{Na}]_{G(w)}$ = Concentration in groundwater of Sodium originating from weathering (μmolL^{-1}).

If we assume that dissolved Na is conservative in the system, we can write:

$$\frac{[\text{Na}]_R}{[\text{Cl}]_R} = \frac{[\text{Na}]_{G(R)}}{[\text{Cl}]_G} = \frac{[\text{Na}]_G - [\text{Na}]_{G(w)}}{[\text{Cl}]_G} \quad (4)$$

where $[\text{Na}]_R$ = Sodium concentration in rain (μmolL^{-1})

The concentration in groundwater of Sodium originating from weathering $[\text{Na}]_{G(w)}$ can hence be estimated from Eqs. 3 and 4 as:

$$[\text{Na}]_{G(w)} = [\text{Na}]_G - [\text{Na}]_R \frac{[\text{Cl}]_G}{[\text{Cl}]_R} = [\text{Na}]_G - [\text{Na}]_R \text{CF} \quad (5)$$

Finally, if we consider that the production of Na by plagioclase weathering takes place mostly in the root zone, i.e. soil and shallow saprolite⁵¹, the concentration factor due to ET will be the same as for Na inputs from rain. Therefore, we can estimate the input concentration of Sodium originating from weathering $[\text{Na}]_w$ (μmolL^{-1}) as follow:

$$[\text{Na}]_w = \frac{[\text{Na}]_{G(w)}}{\text{CF}} \quad (6)$$

In agrosystems, Cl is not only added by rain but also often by fertilizers, mostly in the form of KCl. Cl and Na concentrations in groundwater can be decomposed as:

$$[\text{Cl}]_G = [\text{Cl}]_{G(R)} + [\text{Cl}]_{G(F)} \quad (7)$$

$$[\text{Na}]_G = [\text{Na}]_{G(R)} + [\text{Na}]_{G(w)} \quad (8)$$

where $[\text{Cl}]_{G(F)}$ = Chloride concentration in groundwater originating from fertilizer input (μmolL^{-1})

If we assume that $[\text{Na}]_w$ is similar in the natural system and the agrosystem and that the concentrations of Na originating from rain and weathering are affected similarly by evapotranspiration, we can use the average value of $[\text{Na}]_w$ found in the natural system to estimate CF for each tubewell in the agrosystems as:

$$\text{CF} = \frac{[\text{Na}]_G}{[\text{Na}]_R + [\text{Na}]_w} \quad (9)$$

Assuming that both dissolved Cl and Na are conservative, we can write:

$$\frac{[\text{Na}]_R}{[\text{Cl}]_R} = \frac{[\text{Na}]_{G(R)}}{[\text{Cl}]_{G(R)}} \quad (10)$$

which is equivalent to

$$[\text{Cl}]_{G(R)} = [\text{Na}]_{G(R)} \frac{[\text{Cl}]_R}{[\text{Na}]_R} \quad (11)$$

Using the above equations, we can calculate the contribution of rain $[\text{Cl}]_{G(R)}$ and fertilizers $[\text{Cl}]_{G(F)}$ to the Cl concentration in GW as:

$$[\text{Cl}]_{G(R)} = ([\text{Na}]_G - [\text{Na}]_{G(w)}) \frac{[\text{Cl}]_R}{[\text{Na}]_R} = ([\text{Na}]_G - [\text{Na}]_w \text{CF}) \frac{[\text{Cl}]_R}{[\text{Na}]_R} \quad (12)$$

$$[\text{Cl}]_{G(F)} = [\text{Cl}]_G - [\text{Cl}]_{G(R)} \quad (13)$$

Finally, we can also calculate $[\text{Cl}]_F$ (μmolL^{-1}), being the input concentration of Chloride originating from fertilizers, i.e. without the concentrating effect of evapotranspiration, as follow:

$$[\text{Cl}]_F = \frac{[\text{Cl}]_{G(F)}}{\text{CF}} \quad (14)$$

For the deconvolution method to be applicable, three main assumptions have to be verified, 1) dissolved Na and Cl are conservative 2) their concentrations are affected similarly by evapotranspiration and 3) mineral weathering rates in agricultural catchments can be deduced from neighbouring pristine catchments. In this study, we assessed these assumptions in the case of an agricultural catchment in South India (Berambadi) by:

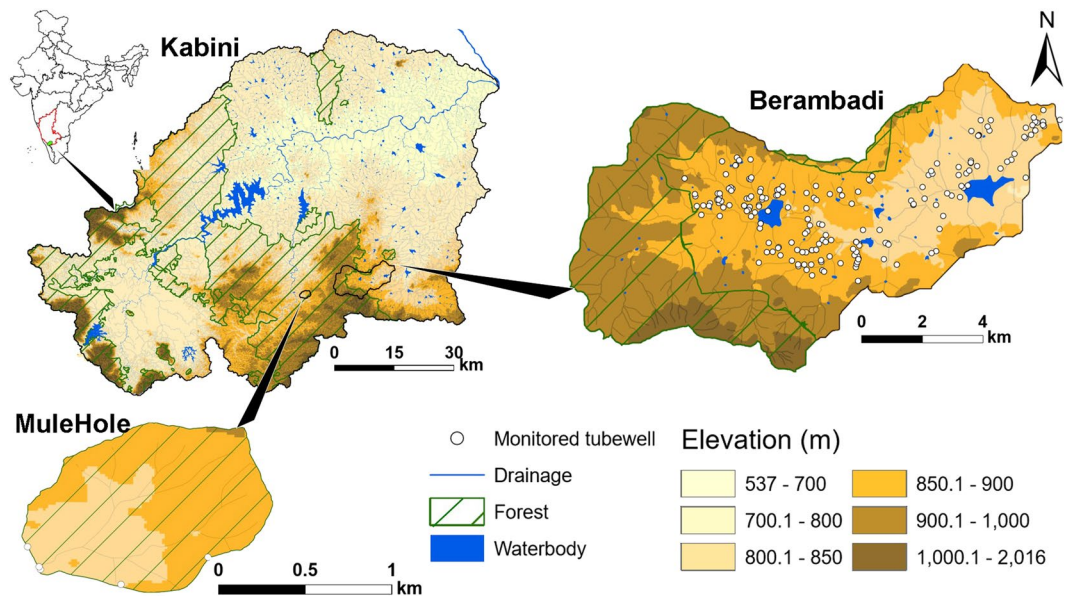


Figure 1. Elevation map of Kabini basin, which includes the Mulehole forested pristine catchment and Berambadi cultivated catchment, showing the density of monitored tube wells (maps were generated using ArcGIS version 10.3.0, <https://desktop.arcgis.com/en/>).

- (1) Using previous studies in the site suggesting that Chloride and Sodium are conservative in this system and likely to be similarly affected by evapotranspiration.
- (2) Testing the assumption that the release of Na in groundwater by Na-plagioclase weathering occurs with the same intensity in both catchments (i.e. $[Na]_w$ is similar). Indeed, variations in plagioclase weathering across wells and sites might occur due to differences in local composition of the bedrock, regolith thickness, residence time of the water in the vadose zone, and the aggressiveness of the groundwater⁵³. To assess the variability in weathering rates between the two catchments, we used Europium, a Rare Earth Element which is more concentrated in plagioclase compared to the other REE. Its relative enrichment in groundwater with respect to its neighbouring REEs, Sm and Gd, induces a positive Europium anomaly (further notes as Eu*) and can be used as a proxy of relative plagioclase weathering in the vadose zone^{54,55}. We compared the positive Eu-anomaly in the groundwater of both pristine and cultivated systems, assuming that a similar average and variability of the positive Eu-anomaly in groundwater for both sites would indicate a similar Na production by plagioclase weathering.

Finally, to assess the robustness of the method, we assess its sensitivity to the $[Na]_w$ value used for the deconvolution in the agrosystems, using a range corresponding to the variability observed in the pristine catchment.

Study Area

The deconvolution method was applied in the Kabini Critical Zone Observatory⁵⁶ (M-TROPICS, part of OZCAR research infrastructure) in Southern India. The Observatory comprises the agricultural catchment of Berambadi and the neighboring pristine catchment of Mule Hole (Fig. 1). The main characteristics of the observatory are described in⁴⁹.

The climate is tropical sub-humid. The monsoon dynamics drives three main seasons: Summer (dry season, from January to May), Kharif (South-West monsoon season, June to September) and Rabi (North-East monsoon season, from October to December). Rainfall patterns display broad decennial trends as well as strong inter-annual variability⁵⁷ with recurrence of droughts⁵⁸. The bedrock of both catchments consists in Precambrian gneiss with few patches of amphibolite, with a two layers aquifer: a regolith, composed of an immature saprolite (on average 15 m thick²³; topped by a 2 m thick ferralsol/vertisol system⁵⁹ and below a fissured zone located in the fresh bedrock. This structure is typical of a hard rock aquifer^{60,61}. Vertisols are predominantly found in valley bottoms. Both saprolite and soils contain residual primary minerals like quartz, Na-plagioclase and sericite and secondary minerals like Fe-oxyhydroxides and clay minerals.

The pristine, forested catchment of Mule Hole. The Mule Hole catchment (4.1 km²) is located 11°43'N–76°26'E, about 10 km at the west of the Berambadi catchment, in the sub-humid zone of the climatic gradient induced by the western Ghats. This forested catchment is part of the Bandipur National Park and then preserved from any anthropogenic activity since at least the creation of the sanctuary in 1974. Long term annual rainfall ranges from 800 to 1500 mm/yr with an average of 1100 mm/yr. Vegetation consists of a dry deciduous forest dominated by the “ATT” facies, i.e. *A. latifolia*, – *T. grandis* and *T. alata* with *T. triandra* grass (Elephant grass)⁵¹. This experimental catchment is monitored for meteorological, hydrological and geochemical variables since 2003 for assessing, from decennial hydrological and geochemical budgets, the processes governing

soil-plant-water interactions. Water mass balance indicates that evapotranspiration accounts for 80 to 90% of the water budget. As a consequence, the forest mediates through the water stock in the vadose zone, the groundwater recharge and discharge and the stream fluxes^{19,62}. By combining the SVAT model COMFORT⁶² with the observations of tree growth, we recently established that co-dominant tree species (among which ATT species) display distinct root uptake depths, indicating that competition drives hydrological niche separation⁶³. Deep root uptake explains the long residence time of water in the vadose zone of the forest, up to 20 years according to the COMFORT model⁴⁷, depending on saprolite thickness and water content.

The cultivated catchment of Berambadi. In the Berambadi catchment (84 km²) the climate is slightly drier than in Mule Hole. The average rainfall is 800 mm/year with a slight gradient from West to East from 900 to 750 mm/year. Most of the rainfall occurs during the southwest monsoon from June to September. Potential evapotranspiration is 1100 mm (aridity index P/PET of 0.7). Agricultural cropland and forest cover are the major land use in the catchment with 52% and 32%, respectively⁶⁴. The development of tube well irrigation since 30 years has induced a shift from the rainfed to irrigated agriculture. As a result, the area with high water demanding cash crops (Turmeric, Banana, Sugarcane) increased at the expense of traditional rainfed crops such as finger millet, pulses etc. As groundwater availability for irrigation is limited by the low transmissivity of the aquifer, and by the fact that electricity for submersible pumps, although freely provided by the government, is only available for 3–4 h/day, the tube well density is increasing in the catchment³⁷. About 5000 farms exist in the catchment, with an average size of about 1 ha, divided into cultivated plots with an average size of 0.2 ha^{64,65}. This led to a large diversity of agricultural practices, depending on crop and farm types. The diversity of farming systems across the catchment was characterized as three main farm types: High productive farms, small and marginal rainfed farms and small irrigated farms⁶⁵.

Materials and Methods

Catchment monitoring and sampling. In the Mule Hole sub-catchment, we used 5 piezometers, drilled in 2003 and 2004 and located along the catchment boundaries, while in the Berambadi catchment we used 188 farmer's tube wells (Fig. 1). Depths to groundwater (distance from ground surface to groundwater table static level, expressed in meter below the surface) was measured with a manual piezometric level sensor (skinny dipper device, Haron instruments). In the Berambadi catchment, measurements were done at least 10 hours after pumping stops, to allow water table to recover from drawdown and approach static level. In Mule Hole we collected the 5 piezometers on monthly basis from 2005 to 2018 while in Berambadi we sampled once the 188 tube wells, between 25th to 28th April 2014.

Chemical analyses. Conductivity and pH were determined in the field using a WTW meter. Each sample was filtrated in the field and stored in two pre-cleaned polypropylene bottles. The first bottle, not acidified, was used for determination of major dissolved species. Anions and cations were measured with an Ion Chromatograph Metrohm 861. Silica concentration was determined using the molybdate blue method with a UV- visible Knauer detector. The accuracy of analyses was controlled with multiple Certified Reference Materials (AnionWS, ION-96.4, ION 915, SUPER-05, BIG MOOSE 02 and PERADE) depending on the range of concentrations. Alkalinity was determined with the alkalinity titrator Mettler Toledo-DL50 Rondolino. Usual precision obtained on major dissolved species determination was about 5%. Whole accuracy was also checked using NICB (Normalized Inorganic Charge Balance⁶⁶). The other bottle was acidified onsite with bi-distilled nitric acid for determination of trace elements concentrations (including Al and Rare Earth Elements) with an Agilent 6000 quadripolar ICPMS at Geosciences Environment Toulouse (France). Accuracy of analyses was checked with SLRS 5 reference materials. Overall precision on trace element analyses was about 10%.

Calculation of indices and mapping. The degree of pollution of groundwater was calculated according to the definition of⁶⁷ which is based on the relative proportion of anions of possible anthropogenic origin compared to the whole anionic charge:

$$\% \text{ pollution} = \frac{[\text{Cl}^-] + [\text{SO}_4^{2-}] + [\text{NO}_3^-]}{[\text{Cl}^-] + [\text{SO}_4^{2-}] + [\text{NO}_3^-] + [\text{Alkalinity}]} * 100 \quad (15)$$

where all the concentrations are in $\mu\text{eq/L}$.

The Europium anomaly (Eu^*) is a proxy for plagioclase weathering^{54,55}. It is calculated by normalization of its concentration by those of his neighbours (Sm & Gd) and to the average gneissic bedrock²³ according to the equation:

$$\text{Eu}^* = \frac{\frac{\text{Eu}_{\text{GW}}}{\text{Eu}_{\text{bedrock}}}}{\left(\frac{\text{Sm}_{\text{GW}}}{\text{Sm}_{\text{bedrock}}}\right)^{0.5} \cdot \left(\frac{\text{Gd}_{\text{GW}}}{\text{Gd}_{\text{bedrock}}}\right)^{0.5}} \quad (16)$$

The saturation index of groundwater regarding Na-plagioclase (albite) was calculated using the PHREEQC software⁶⁸. Catchment water quality maps were constructed by interpolation of the borewell observation data using kriging and an exponential variogram model – characterizing the spatial dependence of the variability in MATLAB⁶⁹ and displayed with ArcGIS version 10.3.0. It should be noted that uncertainty increases towards the boundaries of the mapped area.

Map of irrigation distribution was constructed from the results of^{64,70}. These authors used multi-temporal Landsat satellite images from the year 1990 to 2016. Details of the methods can be found in their paper. In brief,

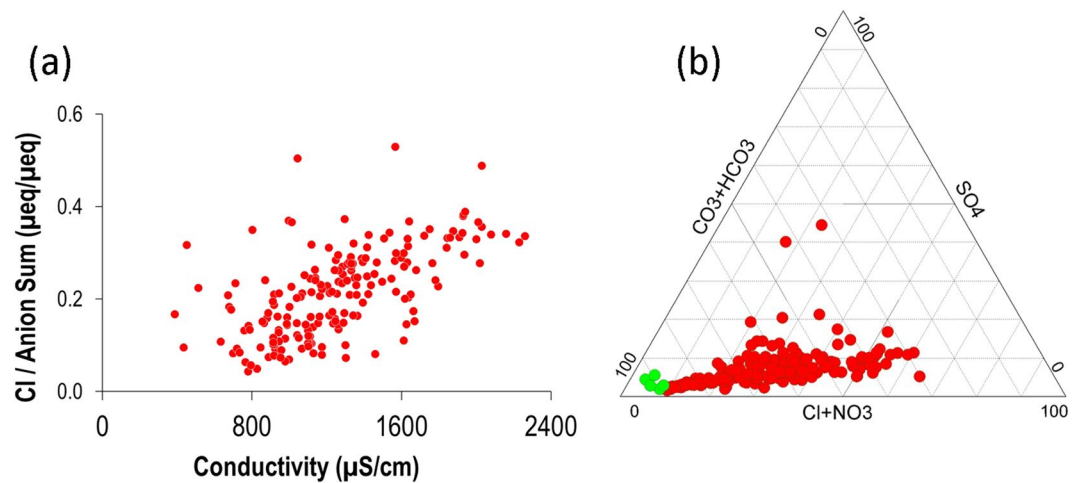


Figure 2. (a) Relationship between conductivity and relative proportion of chloride in Berambadi groundwater, (b) Evolution of anion composition from bicarbonate-dominated waters in the pristine end-member (Mule Hole, green dots) to Cl- and NO_3^- -dominated waters in Berambadi (red dots).

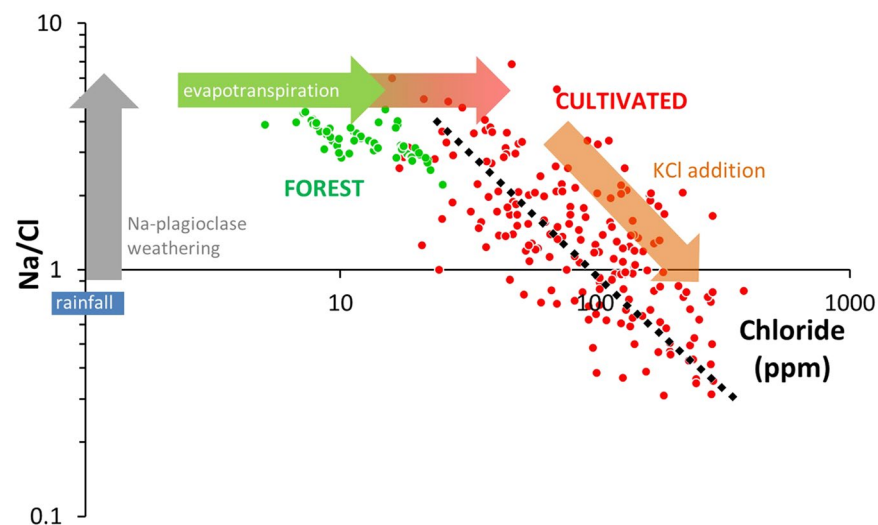


Figure 3. Relationship between Cl concentration and Na/Cl molar ratio in Berambadi (red dots) and Mule Hole (Green dots) groundwater. Dashed black line correspond to theoretical evolution of Na/Cl and Cl concentration if KCl is added to a pristine water. For clarity, only samples collected in 2014 in the Mule Hole catchment are shown.

the irrigated area and non-irrigated classification were performed with Support vector machine algorithm using EVI, NDMI, and NDVI indices. The irrigated and non-irrigated croplands were estimated for the rabi and summer season at an interval of 5 years with high classification accuracy (kappa coefficient greater than 0.9). No analysis was done during the monsoon (kharif) as it is mostly cloudy. In this paper, based on these data, we recomputed the map of irrigation distribution corresponding to the period anterior to the sampling date (1990–2013).

Results

Groundwater quality. In the pristine catchment of Mule Hole, conductivity ranges from 300 to 900 $\mu\text{S/cm}$ and it is lithology controlled^{23,71}. Highest conductivities are located in amphibolite bedrock, but the occurrence of this lithology is not frequent (7%) in this gneiss-dominated catchment. pH is neutral and rather homogeneous across the catchment (7.06 ± 0.2). Cation composition is dominated by Na and Ca. The cationic charges are mainly balanced by alkalinity, which accounts for up to 90% of anionic charges and to a lesser extent by chloride. Pollution Index was $11 \pm 3\%$ which is consistent with the pristine characteristics of Mule Hole.

In contrast, about 90% of Berambadi groundwater samples exhibit conductivities between 700 and 2000 $\mu\text{S/cm}$. Extreme values reach 2300 $\mu\text{S/cm}$, similar to those observed in the semi-arid part of the upper Cauvery Basin⁷². The anionic composition evolves as the conductivity increases, with an increase of Cl proportion (Fig. 2a) at the expense of alkalinity (Fig. 2b). Contrary to anions, none of the relative cation concentrations increases with

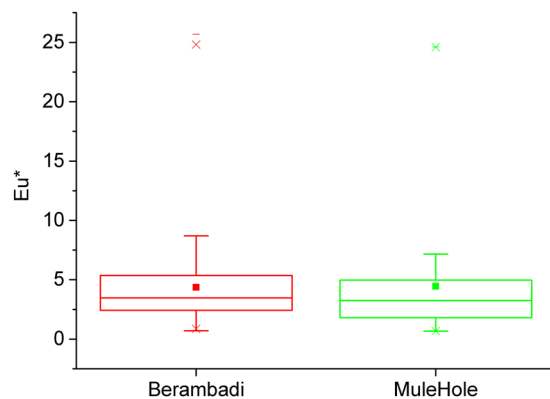


Figure 4. Europium anomaly variation in Berambadi and Mulehole groundwater.

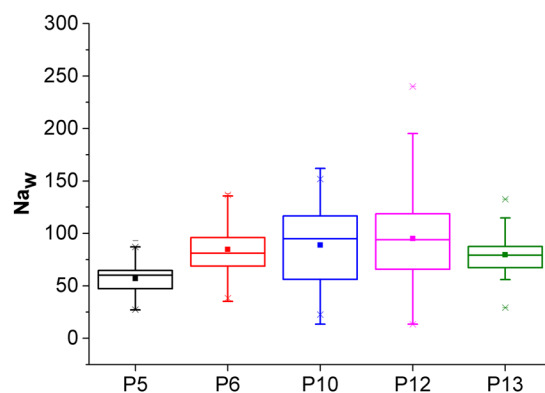


Figure 5. $[Na]_w$ in the groundwater of the pristine catchment of Mule Hole. Bars correspond to the temporal variability of water composition in each piezometer (2006–2017).

conductivity (not shown). For a majority of samples, the cationic load is dominated by Na, followed by Ca and Mg. Potassium, although massively applied as fertilizer, never accounts for more than 2% of the cationic load. No relationships were found between conductivity and the concentration of any specific cations. Pollution index spans a large range of values, from 10% (similar to those of Mule Hole) to 75%, and displays a weak positive correlation with electrical conductivity ($R^2 = 0.34$; not shown).

The comparison between Na/Cl molar ratio and Cl concentration of groundwater samples (Fig. 3) reveals a contrasted pattern between pristine and agricultural catchments, which is in accordance with the assumptions on the processes controlling the relative evolution of Na and Cl in the groundwater posed in section 2.

In Mule Hole, local precipitations exhibit an average Na/Cl molar ratio close to the seawater value (0.85) and Cl concentration around 1 ppm⁵¹. Once infiltrated into the vadose zone, Cl concentration rises due to evapotranspiration only, while Na concentration also rises due to Na-plagioclase weathering. As a consequence, the Na/Cl molar ratio in groundwater increases to reach an average of 3.5 ± 0.98 . In Berambadi, for groundwater sample with similar Na/Cl ratios as in Mule Hole, the Cl concentration is higher, suggesting a higher rate of evapotranspiration. In addition to the above processes, KCl addition leads to an increase of Cl concentration and a concomitant decrease of the Na/Cl ratio down to 0.3.

The average and standard deviations of the Europium anomaly Eu^* (Fig. 4) in groundwater are similar in Mule Hole (4.0 ± 4.6) and in Berambadi (4.4 ± 3.3) despite Na concentration being on average larger by a factor 4 in Berambadi compared to Mule Hole. This suggests that plagioclase weathering rates are similar in both catchments, and therefore the input concentration of Sodium originating from weathering $[Na]_w$ estimated in Mule Hole can be used to apply the deconvolution method in Berambadi.

Deconvolution method. In the Mule Hole forest, the concentration factor due to evapotranspiration (CF) calculated from Eq. (1) was 12.3 ± 5.64 . This is consistent with the water balances calculated for this catchment^{19,62}. The variability is probably due to variations in regolith depth and vegetation cover. Estimated $[Na]_w$ was $80.72 \pm 31.5 \mu\text{molL}^{-1}$ and the spatial variability between piezometers was small compared to the temporal variability for each piezometer (Fig. 5). This suggests that plagioclase weathering depends more on temporal variations in residence time of water in the vadose zone than on the heterogeneity in bedrock composition⁴⁷.

In the tubewells of the Berambadi catchment, using the average value of $[Na]_w$ estimated in Mule Hole from Eq. 6, estimated CF was 34.7 ± 21.09 , i.e. on average about 3 times more than in the natural system and with larger

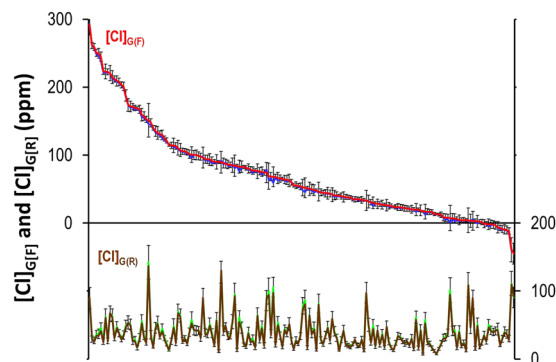


Figure 6. Contribution of rain $[Cl]_{G(R)}$ (brown line) and fertilizers $[Cl]_{G(F)}$ (red line) to the Cl concentration in groundwater in each tube wells of the Berambadi Catchment (ranked by decreasing $[Cl]_{G(F)}$) calculated using the average $[Na]_w$ in the forested catchment. The blue and green lines show respectively the average of $[Cl]_{G(R)}$ and $[Cl]_{G(F)}$ calculated using 20 random values spanning the range of the natural variability $[Na]_w$ and error bars show the standard deviation.

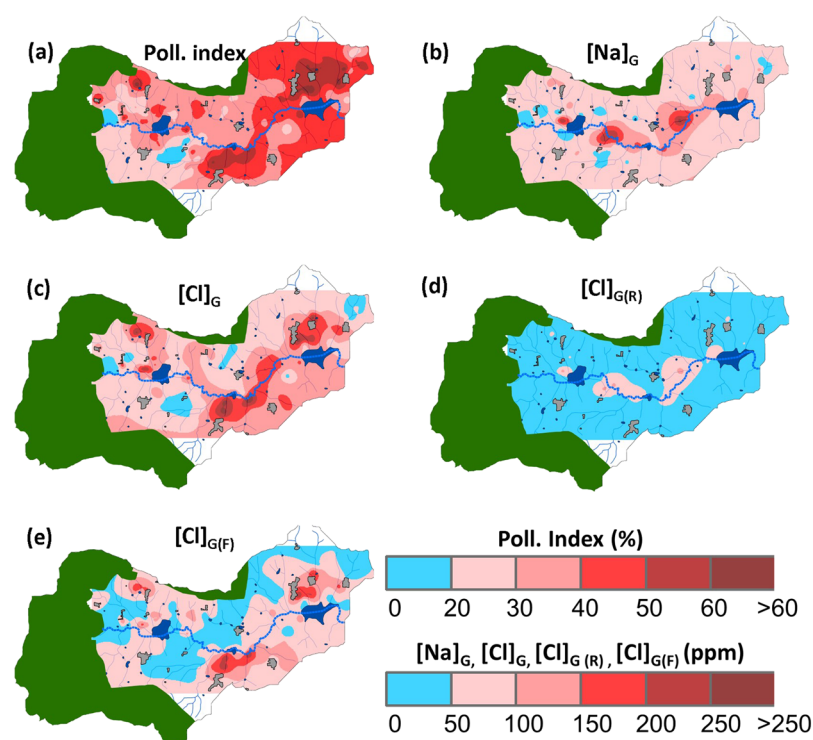


Figure 7. Spatial distribution of groundwater quality in the Berambadi catchment: (a) pollution index, concentration (ppm) in groundwater of (b) Sodium, (c) Chloride, (d) Contribution of rain $[Cl]_{G(R)}$ and (e) fertilizers $[Cl]_{G(F)}$. The green, dark blue and grey colours show forest, ponds and settlements respectively, the dotted blue line shows the main stream (maps were generated using ArcGIS version 10.3.0, <https://desktop.arcgis.com/en/>).

variability. We can explain this variability by the diversity in farming systems, with rainfed systems likely to have a low CF while irrigated systems likely to have high CF, because of longer duration crops and groundwater recycling.

We deconvoluted Cl sources for the 188 tubewells of Berambadi using Eq. 12 for $[Cl]_{G(R)}$ and Eq. 13 for $[Cl]_{G(F)}$ and found that the average contribution of rain to the Cl concentration in groundwater $[Cl]_{G(R)}$ was 38.1 ± 23.2 ppm, while the average contribution of fertilizers $[Cl]_{G(F)}$ was 71.6 ± 67.78 ppm, i.e about 60% of the total concentration. Tubewells span a broad range of $[Cl]_{G(F)}$ values from zero to 300 ppm (Fig. 6). While only 3% of the tubewells displayed slight negative values, suggesting that $[Na]_w$ used in the analysis was not overestimated, 27% were above 100 ppm and could be noted as “hot spots”. We performed a sensitivity analysis by using the deconvolution method for each tube well using 20 random $[Na]_w$ values between 50 and $110 \mu\text{molL}^{-1}$, that corresponds to the standard deviation of the natural variability observed in Mule Hole. The resulting variation of $[Cl]_{G(F)}$ for each tubewell (error bars in Fig. 6) was small compared to the total range of variation, suggesting that

the uncertainty in $[\text{Na}]_w$ estimation is not likely to affect much the ranking of tubewells. It is noteworthy that $[\text{Cl}]_{\text{G(R)}}$ and $[\text{Cl}]_{\text{G(F)}}$ were not correlated, suggesting that variations in evapotranspiration are not the main/sole factor controlling the occurrence of hot spots of $[\text{Cl}]_{\text{G(F)}}$.

Spatial variability of groundwater quality. If groundwater quality displays large small-scale spatial heterogeneity, yet patterns can be observed at the landscape scale (Fig. 7). The pollution index (Fig. 7a) is increasing from the West, where values are close to those found in the pristine watershed, to the East where it is generally above 50%, with a hot spot close to the outlet. This latter area was identified as a vulnerable zone by³⁷ due to the combination of groundwater depletion, low hydraulic gradient and intensive agricultural practices. It was also in the same area that significant impact of salinity on crop yield has been identified³⁸. Na concentrations (Fig. 7b) were rather homogeneous, with hotspots located only along the main valley bottom. The spatial pattern of groundwater total Chloride concentration (Fig. 7c) is similar to the one of the Pollution Index, confirming that Chloride is a marker of groundwater quality degradation. The contribution of rain $[\text{Cl}]_{\text{G(R)}}$ to Cl groundwater concentration is overall low (Fig. 7d). Largest values occur only in the valley bottoms, suggesting that these zones are prone to higher evapotranspiration rates. To the contrary, the contribution of fertilizers $[\text{Cl}]_{\text{G(F)}}$ is higher on the hillslopes, with several hot spots (Fig. 7e).

Discussion

Our analysis of the high-density tubewell sampling in the Berambadi agricultural catchment shows that the groundwater chemical composition displays high values of Chloride concentrations with a high small-scale spatial variability. In the following sections we first discuss the deconvolution method validity and robustness, then, the processes controlling the variability of concentration factor and Chloride sources in Berambadi. Finally, we highlight some implications of our findings for mitigating the observed incipient groundwater salinization.

Validity assessment of deconvolution method. The deconvolution method we introduced for deconvoluting Chloride concentrations in groundwater using Na as a reference is based on three main assumptions: (1) dissolved Na and Cl are conservative, (2) they are subjected to the same concentration factor due to ET and 3) the release of Na by plagioclase weathering is similar for the pristine and the agricultural catchments.

Na and Cl are conservative. It is widely accepted that Chloride behaviour in catchments is conservative⁵² except in the presence of evaporite mineral formations. For Na, different processes can lead to non-conservative behaviour, and must be checked for specific sites. In our study site, previous studies demonstrated that Na is not recycled in any secondary mineral during weathering processes²³ and only marginally adsorbed onto clays contrary to the other major cations Ca, Mg, K⁷³. It was also recently demonstrated in the case of Mule Hole that Na was not significantly cycled through the vegetation^{47,51}. This supports the absence of reactive behaviour of Na once in solution. In Berambadi, the same conservative behaviour is expected as the pedoclimatic and geological conditions are similar.

Concentration factor due to evapotranspiration is same for all Cl and Na sources. It is reasonable to assume that the concentration factor will be same for both sources of Cl, as both rain and fertilizers inputs are applied at the soil surface, and preferential flow is not likely to be significant in the study site context. For Na, while rain input is applied at the surface, inputs from weathering can occur at different depths. However, in the forested pristine catchment of Mule Hole it was recently demonstrated that plagioclase weathering occurs mostly in the soil and secondarily in the shallow underlying saprolite⁵¹ because the aggressiveness of solutions regarding primary silicate minerals decreases as solutions percolate in depth²³. Evapotranspiration is also mostly happening in the soil layer and the shallow saprolite, as only few deep-rooted tree species access the deep vadose zone⁶³, we can reasonably assume that in the forested pristine catchment, Na produced by weathering is subjected to similar CF as the rain inputs.

In contrast, in the agricultural context, characterized by shallow rooted crops, the sodium released by weathering below the root zone is not directly affected by evapotranspiration. However, larger evapotranspiration rate combined with recycling of groundwater for irrigation implies that the solutions infiltrating below the root zone are closer to saturation with respect to silicate minerals than in the forested watershed, and then less aggressive towards silicate minerals. As a consequence, the fraction of sodium released by weathering below the root zone is likely to be small. Neglecting it in Eq. 9 would lead to a slight underestimation of CF and subsequently a slight overestimation of $[\text{Cl}]_{\text{G(F)}}$. In the present study, this possible bias may not have a large impact considering the range of $[\text{Cl}]_{\text{G(F)}}$ found (Fig. 6), with a significant number of tubewell displaying $[\text{Cl}]_{\text{G(F)}}$ values close to zero. In fact, in such groundwater irrigated systems, this bias is likely to be compensated by the additional evapotranspiration occurring during the multiple recycling of groundwater.

Similar release of Na by plagioclase weathering in pristine and agricultural catchments. The similar range of Eu* anomaly found in groundwater of both catchments suggests that plagioclase weathering intensity are similar in the pristine and the agricultural catchment. This might seem surprising as differences in weathering intensity are expected when groundwater residence time or to water aggressiveness are different. The residence time of water in the weathered zone is long in the forested catchment, because the significant water uptake by tree roots in the saprolite buffers groundwater recharge processes^{62,63}. It ranges between 2 to more than 20 years depending on the saprolite thickness⁴⁷. In Berambadi, plant uptake is limited to the root zone of crops and therefore the residence time of water in the vadose zone is likely to be shorter, not more than a few years. However, recycling

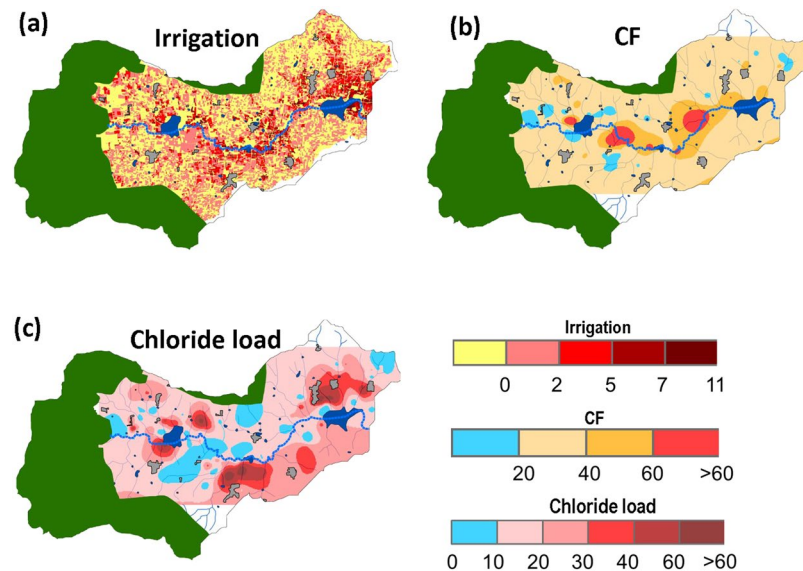


Figure 8. Spatial variations of (a) number of irrigation occurrences from 1990 to 2013 using satellite imagery (See methods) (b) Concentration factor due to evapotranspiration (CF, dimensionless) in the Berambadi catchment and (c) Chloride load ($\text{kg Cl. ha}^{-1} \cdot \text{y}^{-1}$) originating from fertilizers. The green, dark blue and grey colours show forest, ponds and settlements respectively, the dotted blue line shows the main stream (maps were generated using ArcGIS version 10.3.0, <https://desktop.arcgis.com/en/>).

of groundwater for irrigation increases the residence time of water and probably compensate at least partly the difference between the two catchments.

Weathering rates have been found to be higher in agricultural catchments than in pristine ones in temperate humid climate, mostly due to the acidification of soil pore water induced by large inputs of nitrogen fertilizers⁵³. In Berambadi, groundwater pH is neutral and rather homogeneous across the catchment -even in nitrate-rich groundwater, because pore water solutions are buffered by the carbonate minerals in the regolith^{73,74} and in the bedrock²³. Therefore, we can assume that fertilizer application does not significantly impact the intensity of plagioclase weathering in the catchment. Saturation indices calculated for each tube well using PHREEQC software (Fig. S1) show that while groundwater in Mule Hole is undersaturated with respect to albite (-2.5 ± 1), in Berambadi it is near equilibrium (-0.8 ± 0.6). According to⁷⁵, plagioclase dissolution rate remains constant when saturation index varies between -4 to -0.5 , supporting the assumption that Na_w estimated in the forest can be used for most of tube wells in the agricultural catchment. The spatial distribution of saturation index (Fig. S1) reveals that only few spots display saturation index beyond -0.5 , mostly in the valley bottoms. Interestingly, these hot spots do not match the Na concentration ones (Fig. 7b). In locations with SI close to 0, the current plagioclase weathering rates could be limited. If this is the case, using the average Na_w estimated in the pristine catchment in these few locations would lead to an underestimation of CF and therefore an overestimation of the Cl added by fertilizers. However, the groundwater with high SI values did not display Eu-anomalies significantly different from those with low values, suggesting that average weathering rates were not different in these locations.

Importantly, we have shown that the deconvolution method was little sensitive to the estimated Na release from Na-plagioclase weathering (Fig. 3) mostly because, in the study case, Cl concentrations spanned over about 2 orders of magnitude, while Na_w variability is much lesser (Fig. 5).

Variability of the concentration factor and sources of Chloride in the agricultural catchment.

The concentration factor in the Berambadi groundwater was on average about 4 times greater than in the nearby forest of Mule Hole, suggesting that the proportion of rainfall contributing to the groundwater recharge is much lesser in the agricultural context. This can be explained on one hand by the lower annual rainfall in Berambadi (~ 800 mm) compared to Mule Hole (~ 1100 mm), and on the other hand by the widespread occurrence of groundwater irrigation across the catchment (Fig. 8a). Indeed, in addition to the enhanced evapotranspiration due to long or multiple crop cycles, groundwater irrigation is likely to induce higher concentration factor due to groundwater recycling³⁴. In few hot spots, all located in the valley bottom along the streambed, the concentration factor was more than 60 (Fig. 8b). These zones are dominated by deep vertisols which low permeability favours intense evapotranspiration. In these soils, deep soil cracks favour high evaporation at depth, which can lead to a “desiccation-crack-induced salinization”⁷⁶. However, in Berambadi, the largest concentrations of Cl originating from rain inputs ($[\text{Cl}]_R$) were only about 150 ppm (Fig. 7d), which is not enough to impact soil and crop health. In the rest of the catchment, $[\text{Cl}]_R$ remains very low, suggesting that rain Cl input alone, even in this context of semi-arid agriculture with large CF, would not induce salinization. To the contrary, large Cl concentrations originating from fertilizer inputs ($[\text{Cl}]_{G(F)}$) were widespread in the hillslopes, with values up to 290 ppm (Fig. 7e).

The average relative contribution of $[\text{Cl}]_{G(F)}$ to the groundwater concentration of the tubewells was 60%. Considering that average rainfall in Berambadi is 800 mm with Cl concentration of 1 ppm, the annual load from

rainfall is about $8 \text{ kg Cl. ha}^{-1} \cdot \text{y}^{-1}$. If this load represents 40% of the total Cl input, we can estimate that the average load from fertilizers was $20.1 \pm 19.9 \text{ kgCl.ha}^{-1} \cdot \text{y}^{-1}$, with a range between 0 and $90 \text{ kg Cl. ha}^{-1}\text{yr}^{-1}$. The spatial distribution of fertilizer load (Fig. 8c) shows that the practice of applying KCl fertilizers is widespread, with hot spots occurring in several regions, mostly in the hillslopes. Given the high small-scale spatial heterogeneity of practices and lateral groundwater flow, it is challenging to obtain independent assessment of fertilizer input contributing to individual wells. However, we found that our estimated range of inputs is consistent with available regional statistics: For example, at the scale of Karnataka state⁷⁷ the estimated average K input in cultivated land in 2014–2015 is $32 \text{ kg. ha}^{-1} \cdot \text{y}^{-1}$ (i.e. $29 \text{ kg Cl. ha}^{-1} \cdot \text{y}^{-1}$ as virtually all the K is added in the form of KCl) which is slightly higher than the average input we found in Berambadi. Large variations are also found across cropping systems. For example, the 2001–2002 regional fertilizer statistics in Karnataka⁷⁸ shows that K inputs is two times higher for irrigated crops compared to rainfed crops. This suggests that the incipient salinization we found in the Berambadi catchment, and its high spatial variability, is likely to be representative of the region.

Implications for agricultural management for mitigation of incipient salinization. The Cl concentrations measured in the Berambadi groundwater reach values that are already affecting crop yield. In a recent study in the Berambadi catchment³⁸, observed an inverse relationship between turmeric crop yield and soil pore-water conductivity, itself related to the conductivity of the irrigation groundwater. The results of the deconvolution method can provide useful information on the processes governing this incipient salinization, and help designing adequate mitigation policies.

For example, we showed natural features (namely soil properties) leading to high Concentration Factors induced larger values of Cl concentration in the valley bottoms. Even though the resulting concentrations has not reached threatening values, these zones appear to be very vulnerable to any change in agricultural practice that would either increase CF (such as increasing crop cycles or recycling groundwater for irrigation) or Cl inputs from fertilizers. Therefore, in such context, groundwater irrigation should be limited, or conjunctive use of ground and surface water should be promoted. In any case, addition of any form of fertilizer containing Cl should be strongly discouraged.

To the contrary, in the hillslopes, fertilizer addition is the main source of groundwater salinization, which can reach large values in the context of semi-arid agriculture with relatively high concentration factors due to evapotranspiration and groundwater recycling. In such context, mitigation action focused only on promoting practices that would decrease CF, i.e. either promoting rainfed agriculture or decrease water use efficiency of irrigated systems are unlikely to be successful. Finding alternative to KCl as potassium fertilizer would probably be more efficient. Alternatives, such as potassium silicate minerals (K-feldspar, micas) have been proposed which could both reduce salinization and fertilizer cost for the farmers²⁷. However, research is needed to ensure both their agronomic and economic viability in semi-arid conditions.

Conclusion

In this paper, we proposed a methodology to estimate the relative contribution of rainfall vs fertilizer addition to the total Cl concentration in groundwater and quantify the Concentration Factor due to evapotranspiration, using a neighbouring pristine catchment as a reference. We tested the validity of the deconvolution method in our study case by assessing the underlying assumptions, using previous studies in the same site and a geochemical proxy (Eu anomaly). We also assessed the robustness of the method by evaluation the error due to the uncertainty in weathering rate estimation. Applying the deconvolution method to other contexts would require the same careful testing the validity of its underlying assumptions.

We found that Potassium fertilization in the form of KCl is the main source of incipient salinization in the Berambadi catchment. However, sources and processes driving salinization in groundwater were found to vary spatially, with natural features favouring large concentration factor in valley bottoms while fertilization practices being dominant in the hillslopes. These results have strong relevance for designing efficient mitigation policies that should take into account these dominant drivers. The contribution of Cl input by fertilizer to groundwater salinization might vary according to contexts, depending on evapotranspiration intensity and agricultural practices affecting the concentration factor. As groundwater irrigation is fast developing in semi-arid to arid conditions, we expect them to be much more vulnerable to this salinization process than our study site under sub-humid climate. Therefore, we recommend that research on viable alternative forms of K should be urgently engaged to replace the widespread use of KCl for Potassium fertilization in groundwater irrigated semi-arid to arid zones.

Data availability

The datasets generated during and/or analysed during the current study are available from the authors on reasonable request.

Received: 28 August 2019; Accepted: 4 February 2020;

Published online: 28 February 2020

References

1. FAO, The state of the world's land and water resources for food and agriculture (SOLAW) – Managing systems at risk. Food and Agriculture Organization of the United Nations, Rome and Earthscan, London (2011).
2. Suarez, D. L. Impact of agricultural practices on groundwater salinity. *Agric. Ecosystems Environ.* **26**, 215–227 (1989).
3. Pulido-Bosch, A. *et al.* Impacts of agricultural irrigation on groundwater salinity. *Environmental Earth Sciences* **77**(5), 1–14, <https://doi.org/10.1007/s12665-018-7386-6> (2018).
4. Kim, Y. *et al.* Hydrogeochemical and isotopic evidence of groundwater salinization in a coastal aquifer: A case study in Jeju volcanic island, Korea. *Journal of Hydrology* **270**(3–4), 282–294, [https://doi.org/10.1016/S0022-1694\(02\)00307-4](https://doi.org/10.1016/S0022-1694(02)00307-4) (2003).

5. Cardona, A., Carrillo-Rivera, J. J., Huizar-Álvarez, R. & Graniel-Castro, E. Salinization in coastal aquifers of arid zones: An example from Santo Domingo, Baja California Sur, Mexico. *Environmental Geology* **45**(3), 350–366, <https://doi.org/10.1007/s00254-003-0874-2> (2004).
6. De Montety, V. *et al.* Origin of groundwater salinity and hydrogeochemical processes in a confined coastal aquifer: Case of the Rhône delta (Southern France). *Applied Geochemistry* **23**(8), 2337–2349, <https://doi.org/10.1016/j.apgeochem.2008.03.011> (2008).
7. Herczeg, A. L., Dogramaci, S. S., & Leaney, F. W. J. Origin of dissolved salts in a large, semi-arid groundwater system: Murray Basin, Australia. *Marine and Freshwater Research*, **52**(1), 41–52. (2001).
8. Datta, K. K. & Jong, C. D. Adverse effect of waterlogging and soil salinity on crop and land productivity in northwest region of Haryana, India. *Agricultural Water Management* **57**(3), 223–238, [https://doi.org/10.1016/S0378-3774\(02\)00058-6](https://doi.org/10.1016/S0378-3774(02)00058-6) (2002).
9. Scanlon, B. R., Reedy, R. C. & Tachovsky, J. A. Semiarid unsaturated zone chloride profiles: Archives of past land use change impacts on water resources in the southern High Plains. *United States* **43**, 1–13, <https://doi.org/10.1029/2006WR005769> (2007).
10. Williams, W. D. Salinisation: A major threat to water resources in the arid and semi-arid regions of the world. *Lakes & Reservoirs: Research & Management* **4**(3–4), 85–91 (1999).
11. Foster, S. S. D. & Chilton, P. J. Groundwater: The processes and global significance of aquifer degradation. *Philosophical Transactions of the Royal Society B: Biological Sciences*, **358**(1440), 1957–1972, <https://doi.org/10.1098/rstb.2003.1380>.
12. Garduño, H. & Foster, S. Sustainable groundwater irrigation: approaches to reconciling demand with resources. *GWMATE Strategic Overview Series*, Number 4 (2010).
13. Dochartaigh, B. E. Ó. *et al.* Determining groundwater degradation from irrigation in desert-marginal northern China. <https://doi.org/10.1007/s10040-010-0644-7> (2006).
14. Foster, S., *et al.* Impact of irrigated agriculture on groundwater-recharge salinity: a major sustainability concern in semi-arid regions, 2781–2791 (2018).
15. Tyner, J. S., Brown, G. O., Vogel, J. R. & Garbrecht, J. Chloride mass balance to determine water fluxes beneath KCl-fertilized crops. *Transactions of the ASAE* **43**(6), 1553 (2000).
16. Gee, G. W. & Hillel, D. Groundwater recharge in arid regions: Review and critique of estimation methods. *Hydrological Processes* **2**(3), 255–266, <https://doi.org/10.1002/hyp.3360020306> (1988).
17. Subyani, A. M. Use of chloride-mass balance and environmental isotopes for evaluation of groundwater recharge in the alluvial aquifer, Wadi Tharad, western Saudi Arabia, 741–749, <https://doi.org/10.1007/s00254-004-1096-y> (2004).
18. Dettinger, M. D. Reconnaissance estimates of natural recharge to desert basins in Nevada USA using chloride balance calculations. *Journal of Hydrology*, **106** (55–78) (1989).
19. Maréchal, J., Varma, M. R. R., Riotte, J. & Vouillamoz, J. Indirect and direct recharges in a tropical forested watershed: Mule Hole, India, **364**, 272–284, <https://doi.org/10.1016/j.jhydrol.2008.11.006> (2009).
20. Huang, T., Academy, C., Pang, Z. & Academy, C. Estimating groundwater recharge following land-use change using chloride mass balance of soil profiles: A case study at Guyuan and Xifeng in the Loess Plateau of China Estimating groundwater recharge following land-use change using chloride mass balance, (April 2016), <https://doi.org/10.1007/s10040-010-0643-8> (2010).
21. Takounjou, A. F. *et al.* Estimation of groundwater recharge of shallow aquifer on humid environment in Yaounde, Cameroon using hybrid water-fluctuation and hydrochemistry methods. *Environmental Earth Sciences* **64**(1), 107–118, <https://doi.org/10.1007/s12665-010-0822-x> (2011).
22. Velbel, M. A. Geochemical mass balances and weathering rates in forested watersheds of the southern Blue Ridge. *American Journal of Science* **285**(10), 904–930 (1985).
23. Braun, J. J. *et al.* Regolith mass balance inferred from combined mineralogical, geochemical and geophysical studies: Mule Hole gneissic watershed, South India. *Geochimica et Cosmochimica Acta* **73**(4), 935–961, <https://doi.org/10.1016/j.gca.2008.11.013> (2009).
24. Kesler, S. E. *et al.* Na-Cl-Br systematics of mineralizing brines in Mississippi Valley–type deposits. *Geology*, **23**(7), 641, 10.1130/0091-7613(1995)023<0641:ncbsom>2.3.co;2 (1995).
25. Braun, J. J. *et al.* Present weathering rates in a humid tropical watershed: Nsimi, South Cameroon. *Geochimica et Cosmochimica Acta* **69**(2), 357–387, <https://doi.org/10.1016/j.gca.2004.06.022> (2005).
26. Sun, H., Huffine, M., Husch, J. & Sinpatanasakul, L. Na/Cl molar ratio changes during a salting cycle and its application to the estimation of sodium retention in salted watersheds. *Journal of contaminant hydrology* **136**, 96–105 (2012).
27. Manning, D. A. Mineral sources of potassium for plant nutrition. A review. *Agronomy for sustainable development* **30**(2), 281–294 (2010).
28. White, P. J. & Broadley, M. R. Chloride in Soils and its Uptake and Movement within the Plant: A Review, **44**(0), 967–988 <https://doi.org/10.1006/anbo.2001.1540> (2001).
29. Teakle, N. L. & Tyerman, S. D. Mechanisms of Cl-transport contributing to salt tolerance. *Plant, cell & environment* **33**(4), 566–589 (2010).
30. Rhoades, J. D., Corwin, D. L. & Lesch, S. M. Geospatial measurements of soil electrical conductivity to assess soil salinity and diffuse salt loading from irrigation. *Geophysical Monograph Series* **108**(January), 197–215, <https://doi.org/10.1029/GM108p0197> (1998).
31. Pokorny, L., Maturana, I. & Bortle, W. H. Sodium Nitrate and Nitrite. Kirk-Othmer Encyclopedia of Chemical Technology. John Wiley & Sons Inc., New York (2006).
32. Konikow, L. F. Of Long-Term Salinity Changes in an Irrigated Stream-Aquifer System, **21**(11), 1611–1624 (1985).
33. Schmidt, K. D. & Sherman, I. Effect of irrigation on groundwater quality in California. *Journal of irrigation and drainage engineering* **113**(1), 16–29 (1987).
34. Perrin, J., Mascré, C., Pauwels, H. & Ahmed, S. Solute recycling: An emerging threat to groundwater quality in southern India? *Journal of Hydrology* **398**(1–2), 144–154, <https://doi.org/10.1016/j.jhydrol.2010.12.024> (2011).
35. Dharmadhikary, S., Bhalerao, R., Dabadge, A. & Sree Kumar, N. Understanding the Electricity, Water & Agriculture Linkages, 1. Retrieved from [http://www.indiaenvironmentportal.org.in/files/file/Understanding the Electricity, Water & Agriculture Linkages. pdf](http://www.indiaenvironmentportal.org.in/files/file/Understanding%20the%20Electricity,%20Water%20&%20Agriculture%20Linkages.pdf) (2018).
36. Dorin, B. & Aubron, C. Croissance et revenu du travail agricole en Inde. Une économie politique de la divergence (1950–2014). *Economie rurale* **2**, 41–65 (2016).
37. Buvaneshwari, S. *et al.* Groundwater resource vulnerability and spatial variability of nitrate contamination: insights from high density tubewell monitoring in a hard rock aquifer. *Sci. Tot. Env.* **579**, 838–847 (2017).
38. Kizza, T. Model based estimation of turmeric yield response to saline groundwater irrigation. *International Journal of Scientific Research and Engineering Studies*. **3**(10), 8–12 (2016).
39. Cloutier, V., Lefebvre, R., Therrien, R. & Savard, M. M. Multivariate statistical analysis of geochemical data as indicative of the hydrogeochemical evolution of groundwater in a sedimentary rock aquifer system. *Journal of Hydrology* **353**(3–4), 294–313, <https://doi.org/10.1016/j.jhydrol.2008.02.015> (2008).
40. Bouchaou, L. *et al.* Application of multiple isotopic and geochemical tracers for investigation of recharge, salinization, and residence time of water in the Souss-Massa aquifer, southwest of Morocco. *Journal of Hydrology* **352**(3–4), 267–287, <https://doi.org/10.1016/j.jhydrol.2008.01.022> (2008).
41. Vengosh, A., Spivack, A. J., Artzi, Y. & Ayalon, A. Geochemical and boron, strontium, and oxygen isotopic constraints on the origin of the salinity in groundwater from the Mediterranean coast of Israel. *Water Resources Research* **35**(6), 1877–1894 (1999).
42. Singh, A. Review: Computer-based models for managing the water-resource problems of irrigated agriculture. *Hydrogeology Journal* **23**(6), 1217–1227, <https://doi.org/10.1007/s10040-015-1270-1> (2015).

43. Dunne, T. Rates of chemical denudation of silicate rocks in tropical catchments. *Nature* **274**(5668), 244–246 (1978).
44. Négrel, P., Allègre, C. J., Dupré, B. & Lewin, E. Erosion sources determined by inversion of major and trace element ratios and Sr isotopic ratios in river water. The Congo Basin case. *Earth and Planetary Science Letters* **120**, 59–76 (1993).
45. Gaillardet, J., Dupre, B. & Allegre, C. J. Global silicate weathering and CO₂ consumption rates deduced from the chemistry of large rivers. *Chemical Geology* **159**, 3–30 (1999).
46. Gaillardet, J., Dupre, B., Allegre, C. J. & Négrel, P. Chemical and physical denudation in the Amazon River Basin. *Chemical geology* **142**(3–4), 141–173 (1997).
47. Riotte, J. *et al.* Impact of vegetation and decennial rainfall fluctuations on the weathering fluxes exported from a dry tropical forest (Mule Hole). *Proc. Earth Planet. Sci.* **10**, 34–37 (2014b).
48. Riotte, J. *et al.* Processes controlling silicon isotopic fractionations in a forested tropical watershed: Mule Hole Critical Zone Observatory (Southern India). *Geochim. Cosmochim. Acta* **228**, 301–319 (2018).
49. Sekhar, M., Riotte, J., Ruiz, L., Jouquet, P. & Braun, J. J. Influences of Climate and Agriculture on Water and Biogeochemical Cycles: Kabini Critical Zone Observatory. *Proc. Ind. Nat. Sci. Acad.* **82**, 833–846 (2016).
50. Soumya, B. S. *et al.* Inverse models to analyze the spatiotemporal variations of chemical weathering fluxes in a granito-gneissic watershed: Mule Hole, South India. *Geoderma* **165**(1), 12–24 (2011).
51. Riotte, J. *et al.* Vegetation impact on stream chemical fluxes: Mule Hole watershed (South India). *Geochim. Cosmochim. Acta* **145**, 116–138 (2014a).
52. Scanlon, B. R., Reedy, R. C., Gates, J. B. & Gowda, P. H. Impact of agroecosystems on groundwater resources in the Central High Plains, USA Agriculture, ecosystems & environment **139**(4), 700–713 (2010).
53. Pierson-Wickmann, A. C. *et al.* High chemical weathering rates in first-order granitic catchments induced by agricultural stress. *Chemical Geology* **265**(3–4), 369–380, <https://doi.org/10.1016/j.chemgeo.2009.04.014> (2009).
54. Braun, J. J. *et al.* REY-Th-U Solid Dynamics in the Critical Zone: Combined Influence of Reactive Bedrock Accessory Minerals, Authigenic Phases and Hydrological Sorting (Mule Hole Watershed, South India). *Geochemistry, Geophysics, Geosystems* **19**, 1611–1635, <https://doi.org/10.1029/2018GC007453> (2018).
55. Braun, J. J. *et al.* REY-Th-U solute dynamics in the Critical Zone: Combined influence of chemical weathering, atmospheric deposit leaching and vegetation cycling (Mule Hole watershed, South India). *Geochemistry, Geophysics, Geosystems* **18**, 4409–4425, <https://doi.org/10.1002/2017GC007158> (2017).
56. Gaillardet, J. *et al.* OZCAR: The French Network of Critical Zone Observatories. *Vadose Zone Journal* **17**(1), 0, <https://doi.org/10.2136/vzj2018.04.0067> (2018).
57. Sekhar, M., Javeed, Y., Bandyopadhyay, S., Mangiarotti, S. & Mazzega, P. Groundwater management practices and emerging challenges: Lessons from a case study in the Karnataka State of South India. *Groundwater Management Practices*, 436 (2011).
58. Parthasarathy, B., Munot, A. A., & Kothawale, D. R. Theoretical and Applied Climatology All-India Monthly and Seasonal Rainfall Series: 1871–1993, 224, 217–224 (1994).
59. Barbiéro, L. *et al.* Using a structural approach to identify relationships between soil and erosion in a semi-humid forested area, South India. *Catena* **70**(3), 313–329, <https://doi.org/10.1016/j.catena.2006.10.013> (2007).
60. Sekhar, M., Rasmi, S. N., Javeed, Y., Gowrisankar, D. & Ruiz, L. Modeling the Groundwater Dynamics in a Semi-Arid Hard Rock Aquifer Influenced by Boundary Fluxes, Spatial and Temporal Variability in Pumping/recharge. In *Advances in Geosciences: Volume 4: Hydrological Science (HS)* (pp. 173–181) (2006).
61. Dewandel, B., Lachassagne, P., Wyns, R., Maréchal, J. C. & Krishnamurthy, N. S. A generalized 3-D geological and hydrogeological conceptual model of granite aquifers controlled by single or multiphase weathering. *Journal of Hydrology* **330**(1–2), 260–284, <https://doi.org/10.1016/j.jhydrol.2006.03.026> (2006).
62. Ruiz, L., Varma, M. & Muddu, S. Water balance modelling in a tropical watershed under deciduous forest (Mule Hole, India): Regolith matric storage buffers the groundwater recharge process, <https://doi.org/10.1016/j.jhydrol.2009.11.020> (2018).
63. Chitra-tarak, R., Riotte, J., Suresh, H. S., & Sean, M. The roots of the drought: Hydrology and water uptake strategies mediate forest-wide demographic response to precipitation, (April 2017), 1–13, <https://doi.org/10.1111/1365-2745.12925> (2018).
64. Sharma, A. *et al.* Irrigation history estimation using multitemporal landsat satellite images: Application to an intensive groundwater irrigated agricultural watershed in India. *Remote Sensing* **10**(6), 893 (2018).
65. Robert, M. *et al.* Farm typology in the Berambadi Watershed (India): Farming systems are determined by farm size and access to groundwater. *Water* **9**(1), 51 (2017).
66. Edmund, P. Fluvial geochemistry of the eastern slope of the northeastern Andes and its foredeep in the drainage of the Orinoco in Colombia and Venezuela, **60**(16) (1996).
67. Pacheco, F. & Van Der Weijden, C. H. Contributions of water-rock interactions to the composition of groundwater in areas with a sizeable anthropogenic input: A case study of the waters of the Fundo area. *central Portugal* **32**(12), 3553–3570 (1996).
68. Parkhurst D.L. and Appelo C.A.J. Description of input and examples for PHREEQC version 3--A computer program for speciation, batch-reaction, one-dimensional transport, and inverse geochemical calculations: U.S. Geological Survey Techniques and Methods, book 6, chap. A43, 497 p (2013).
69. Trauth, M.H. With text contributions by Gebbers, R. & Marwan, N. MATLAB Recipes for Earth Sciences, 2nd edition, <https://doi.org/10.1007/978-3-540-72749-1> (2007).
70. Sharma, A. K. *et al.* Evaluation of Radarsat-2 quad-pol SAR time-series images for monitoring groundwater irrigation. *International Journal of Digital Earth* **0**(0), 1–21, <https://doi.org/10.1080/17538947.2019.1604834> (2019).
71. Maréchal, J. C., Braun, J. J., Riotte, J., Bedimo, J. P. B. & Boeglin, J. L. Hydrological processes of a rainforest headwater swamp from natural chemical tracing in Nsimi watershed, Cameroon. *Hydrological Processes* **25**(14), 2246–2260 (2011).
72. Soumya, B. S., Sekhar, M., Riotte, J., Banerjee, A. & Braun, J. J. Characterization of groundwater chemistry under the influence of lithologic and anthropogenic factors along a climatic gradient in Upper Cauvery basin, South India. *Environmental earth sciences* **69**(7), 2311–2335 (2013).
73. Violette, A. *et al.* Modelling the chemical weathering fluxes at the watershed scale in the Tropics (Mule Hole, South India): Relative contribution of the smectite/kaolinite assemblage versus primary minerals. *Chemical Geology* **277**(1–2), 42–60, <https://doi.org/10.1016/j.chemgeo.2010.07.009> (2010).
74. Durand, N., Gunnell, Y., Curmi, P. & Ahmad, S. M. Pathways of calcrite development on weathered silicate rocks in Tamil Nadu, India: mineralogy, chemistry and paleoenvironmental implications. *Sed. Geol.* **192**, 1–18 (2006b).
75. Ganor, J., Lu, P., Zheng, Z. & Zhu, C. Bridging the gap between laboratory measurements and field estimations of silicate weathering using simple calculations. *Environmental Geology* **53**(3), 599–610, <https://doi.org/10.1007/s00254-007-0675-0> (2007).
76. Baram, S., Ronen, Z., Kurtzman, D., Külls, C. & Dahan, O. Desiccation-crack-induced salinization in deep clay sediment. *Hydrology and Earth System Sciences* **17**(4), 1533–1545 (2013).
77. Indian Fertilizer scenario 2015. Department of Fertilizer, Government of India, New Delhi (2015).
78. FAI, 2010–2011. Indian Fertilizer statistics. Department of Fertilizer, Government of India, New Delhi (2011).

Acknowledgements

The first author acknowledges the Hydro Nation fellowship provided by the Scottish Government and James Hutton Institute and the INSPIRE fellowship provided by the Department of Science and Technology, Government of India. The study was funded by the project ATCHA ANR-16-CE03-0006, and the Environmental Research Observatory M-TROPICS (<https://mtropics.obs-mip.fr/>), itself supported by the University of Toulouse, IRD and CNRS-INSU. We thank the SUJALA III project team members (Karnataka Watershed Development Department and World Bank) for their support. We also thank the farmers of the Berambadi catchment, Karnataka Forest Department and the staff of the Bandipur National Park for all the support and information provided.

Author contributions

S.B., J.R. and L.R. Conceived the study and wrote the paper. S.B. collected and analysed the agricultural catchment data. S.B. and A.K.S. prepared the tables and figures. M.S., A.K.S., R.H., J.J.B. and M.K.M.S. discussed the results and supervised the findings of this work. All authors reviewed the manuscript.

Competing interests

The authors declare no competing interests.

Additional information

Supplementary information is available for this paper at <https://doi.org/10.1038/s41598-020-60365-z>.

Correspondence and requests for materials should be addressed to S.B.

Reprints and permissions information is available at www.nature.com/reprints.

Publisher's note Springer Nature remains neutral with regard to jurisdictional claims in published maps and institutional affiliations.



Open Access This article is licensed under a Creative Commons Attribution 4.0 International License, which permits use, sharing, adaptation, distribution and reproduction in any medium or format, as long as you give appropriate credit to the original author(s) and the source, provide a link to the Creative Commons license, and indicate if changes were made. The images or other third party material in this article are included in the article's Creative Commons license, unless indicated otherwise in a credit line to the material. If material is not included in the article's Creative Commons license and your intended use is not permitted by statutory regulation or exceeds the permitted use, you will need to obtain permission directly from the copyright holder. To view a copy of this license, visit <http://creativecommons.org/licenses/by/4.0/>.

© The Author(s) 2020